Box-Particle Probability Hypothesis Density Filtering

MAREK SCHIKORA
Fraunhofer FKIE
Germany

AMADOU GNING
University College London
United Kingdom

LYUDMILA MIHAYLOVA, Senior Member, IEEE
University of Sheffield
United Kingdom

DANIEL CREMERS
Technical University of Munich
Germany

WOLFGANG KOCH, Fellow, IEEE
Fraunhofer FKIE
Germany

This paper develops a novel approach for multitarget tracking, called box-particle probability hypothesis density filter (box-PHD filter). The approach is able to track multiple targets and estimates the unknown number of targets. Furthermore, it is capable of dealing with three sources of uncertainty: stochastic, set-theoretic, and data association uncertainty. The box-PHD filter reduces the number of particles significantly, which improves the runtime considerably. The small number of box-particles makes this approach attractive for distributed inference, especially when particles have to be shared over networks. A box-particle is a random sample that occupies a small and controllable rectangular region of non-zero volume. Manipulation of boxes utilizes methods from the field of interval analysis. The theoretical derivation of the box-PHD filter is presented followed by a comparative analysis with a standard sequential Monte Carlo (SMC) version of the PHD filter. To measure the performance objectively three measures are used: inclusion, volume, and the optimum subpattern assignment (OSPA) metric. Our studies suggest that the box-PHD filter reaches similar accuracy results, like an SMC-PHD filter but with considerably less computational costs. Furthermore, we can show that in the presence of strongly biased measurement the box-PHD filter even outperforms the classical SMC-PHD filter.

Manuscript received April 23, 2012; revised October 19, 2012, April 30, 2012, August 8, 2013; released for publication September 20, 2013.

DOI. No. 10.1109/TAES.2014.120238.

Refereeing of this contribution was handled by L. Kaplan.

This work was supported by the European Community's Seventh Framework Program [FP7/2007-2013] under Grant 238710 and by the UK Engineering and Physical Sciences Research Council (ESPRC) via Grant EP /K021516/1.

Authors' addresses: M. Schikora and W. Koch, Department of Sensor Data and Information Fusion, Fraunhofer FKIE, Wachtberg Germany, E-mail: (marek.schikora@fkie.fraunhofer.de); A. Gning, Department of Computer Science, University College London, United Kingdom; L. Mihaylova, Department of Automatic Control and Systems Engineering, University of Sheffield, United Kingdom; D. Cremers Department of Computer Science, Technical University of Munich, Germany.

0018-9251/14/$26.00 © 2014 IEEE

I. INTRODUCTION

Multitarget tracking is a common problem with many applications. In most of these the expected target number is not known a priori, so that it has to be estimated from the measured data. In general, multitarget tracking involves the joint estimation of states and the number of targets from a sequence of observations in the presence of detection uncertainty, association uncertainty, and clutter [1]. Classical approaches such as the joint probabilistic data association filter (JPDAF) [2] and multihypothesis tracking (MHT) [3] need in general the knowledge of the expected number of targets. The finite set statistics (FISST) approach proposed by Mahler [4] is a systematic treatment for multitarget tracking with an unknown and variable number of objects. To reduce the complexity Mahler proposed an approximation of the original Bayes multitarget filter, the probability hypothesis density (PHD) filter. One of the main advantages of the PHD filter is that it avoids the data association problem and resolves the measurement origin uncertainty in an elegant way. In [5, 6] it was shown that the PHD filter outperforms the classical approaches such as the Kalman filter, standard particle filters, and the multiple hypothesis tracking (MHT). Algorithms based on the JPDAF [7] tend to merge tracking results produced by closely spaced objects. This drawback cannot be observed when using the PHD filter. Many implementations of the PHD filter have been proposed, either using sequential Monte Carlo methods (SMC) [8–10], or with Gaussian mixtures [11]. An improved implementation of the SMC-PHD filter was published in [12].

The traditional measurement noise expresses uncertainty due to randomness, often referred to as statistical uncertainty. In many practical applications, however, the standard measurement model is not adequate. Complex distributed surveillance systems, for example, are often operating under unknown synchronization biases and/or unknown system delays. The resulting measurements are affected by bounded errors of typically unknown distribution and biases, and can be expressed rather by intervals than by point values. An interval measurement expresses a type of uncertainty which is referred to as the set-theoretic uncertainty [13, 14], vagueness [15], or imprecision [16]. Some of the first works about representing densities as a mixture of box-particles can be traced back to the early 1970s; see [17] for a review. The concept of box-particle filtering in the context of tracking was introduced in [18]. In [19] it was shown that box-particles could be seen as supports of

uniform probability density functions (pdfs), leading to Bayesian understanding of box-particle filters. In [20] a single target box-particle Bernoulli filter with box measurements is presented.

The main contribution of this work is a general derivation of box-particle methods in the context of multitarget tracking with an unknown number of targets, clutter, and false alarms. We present here a box-particle version of the multitarget PHD filter. In addition, a comparison of the box-PHD filter with a standard SMC-PHD filter is performed. The optimum subpattern assignment (OSPA) metric [21] is used as performance measure, together with the criteria for measuring the inclusion of the true state and the volume of the posterior pdf [20].

The remaining part of this article is structured as follows. A brief introduction to finite set statistics (FISST) is given in Section II. The necessary interval methodology is explained in Section III. Section IV contains a general description of the PHD filter with a basic SMC implementation. The box-PHD filter is derived and described in Section V. Section V-A describes the steps needed to get from point particles to box-particles. A numerical study is presented in Section VI. Conclusions are drawn in Section VII.

II. FINITE SET STATISTICS

In a single-object system, the state and measurement at time k are represented as two random vectors of possibly different dimensions. These vectors evolve in time, but maintain their initial dimension. However, this is not the case in a multiobject system. Here the multiobject state and multiobject measurement are two collections of individual objects and measurements. The number of these may change over time and lead to another dimension of the multiobject state and multiobject measurement. Furthermore, there exists no ordering for the elements of the multiobject state and measurement. Using the theory proposed in [22], the multiobject state and measurement are naturally represented as finite subsets $\mathbf{X}_k$ and $\mathbf{Z}_k$ defined as follows.

Let $N(k)$ be a random number of objects, which are located at $\mathbf{x}_{k,1}, \ldots, \mathbf{x}_{k,N(k)}$ in the single-object state space E_S, e.g. R^d then,

$$\mathbf{X}_k = \left\{\mathbf{x}_{k,1}, \ldots, \mathbf{x}_{k,N(k)}\right\} \in \mathcal{F}(E_S) \tag{1}$$

is the multiobject state, where $\mathcal{F}(E_S)$ denotes the collection of all finite subsets of the space E_S. Analogous to this, we define the multiobject measurement

$$\mathbf{Z}_k = \left\{\mathbf{z}_{k,1}, \ldots, \mathbf{z}_{k,M(k)}\right\} \in \mathcal{F}(E_O), \tag{2}$$

assuming that at the time step k we have $M(k)$ measurements $\mathbf{z}_{k,1}, \ldots, \mathbf{z}_{k,M(k)}$ in the single-object space E_O, which correspond to real targets and clutter. The sets $\mathbf{X}_k$ and $\mathbf{Z}_k$ are also called random finite sets. In analogy to the expectation for a random vector, a first-order moment of the posterior distribution for a random set is of interest here, which is the so-called PHD. The integral value of the PHD over a given region in state space leads to the expected number of objects within this region. Denote $f_{k/k}(\mathbf{x}_k)$ as the PHD associated with the multiobject posterior $p(\mathbf{Z}_k|\mathbf{Z}^k)$ at a time step k, with $\mathbf{Z}^k$ denoting the accumulated measurements from the time steps 1 to k. The PHD filter consists of two steps: prediction and update [4].

The prediction can be realized through the following equation[1]:

$$f_{k|k-1}(\mathbf{x}_k) = b(\mathbf{x}_k) + \int p_s(\mathbf{x}_{k-1}) p(\mathbf{x}_k|\mathbf{x}_{k-1}) f_{k-1|k-1}(\mathbf{x}_{k-1}) \mathrm{d}\mathbf{x}_{k-1}, \tag{3}$$

where $b(\mathbf{x}_k)$ denotes the intensity function of spontaneous birth of new objects, $\mathbf{x}_{k-1}$. $p_s(\mathbf{x}_{k-1})$ is the probability that the object still exists at the time step k given its previous state $\mathbf{x}_{k-1}$, and $p(\mathbf{x}_k|\mathbf{x}_{k-1})$ is the transition probability density of the individual objects. The update equation can be written as

$$f_{k|k}(\mathbf{x}_k) \cong F(\mathbf{Z}_k|\mathbf{x}_k) f_{k|k-1}(\mathbf{x}_k), \tag{4}$$

$$F(\mathbf{Z}_k|\mathbf{x}_k) = 1 - p_D(\mathbf{x}_k) + \sum_{\mathbf{z}\in\mathbf{Z}_k} \frac{p_D(\mathbf{x}_k) p(\mathbf{z}|\mathbf{x}_k)}{\lambda c(\mathbf{z}) + \int p_D(\mathbf{x}_k) p(\mathbf{z}|\mathbf{x}_k) f_{k|k-1}(\mathbf{x}_k) \mathrm{d}\mathbf{x}_k}, \tag{5}$$

where $p_D(\mathbf{x}_k)$ denotes the probability that an object in state $\mathbf{x}_k$ will be detected at time step k. Furthermore, $p(\mathbf{z}|\mathbf{x}_k)$ is the measurement likelihood, $c(\mathbf{z})$ the probability distribution for every clutter point, and λ is the average number of clutter points per scan.

III. INTERNAL ANALYSIS

This section gives a short introduction to the field of interval analysis, which is used in this article. For more information see [23]. The original idea of interval analysis was to deal with intervals instead of real numbers for exact computation in the presence of rounding errors. However, this field has strongly increased its potential applications. We use the main concepts to represent particles not as delta-peaks but as boxes in the state space. An interval $[x] = [\underline{x}, \bar{x}] \in \mathbb{IR}$ is a closed and connected subset of the real numbers $\mathbb{R}$, with $\underline{x} \in \mathbb{R}$ representing its lower bound and $\bar{x} \in \mathbb{R}$ its upper bound. In multiple dimensions d this interval becomes a box $[\mathbf{x}] \in \mathbb{IR}^d$ defined as a Cartesian product of d intervals: $[\mathbf{x}] = [x_1] \times \ldots \times [x_d]$. Here the operator $|[.]|$ denotes the volume of a box $[\mathbf{x}]$. The function mid($[\mathbf{x}]$) returns the center of a box. Elementary arithmetic operations, basic functions, and operations between sets have been naturally extended to the interval analysis context.

[1] Target spawning is not considered in this paper.

For general functions the concept of inclusion functions has been developed. An inclusion function $[\mathbf{g}]$ for a given function $\mathbf{g}$ is defined such that the image of any box $[\mathbf{x}]$ by $[\mathbf{g}]$ is a box $[\mathbf{g}]([\mathbf{x}])$ containing $\mathbf{g}([\mathbf{x}])$. An inclusion function that leads to the smallest box area is needed. Hence, the size of the box $[\mathbf{g}]([\mathbf{x}])$ should be minimal but at the same time has to cover the whole image of a box $[\mathbf{x}]$. An important class in the context of tracking is natural inclusion functions.

DEFINITION 1. Assume $\mathbf{g}: \mathbb{R}^d \to \mathbb{R}, (x_1, \ldots, x_d) \to g(x_1, \ldots, x_d)$ is a function expressed as a finite composition of the operators $+, -, *, /$ and standard mathematical functions (sin, cos, exp, ...). A natural inclusion function is obtained by replacing each real variable and each operator or function by its interval counterpart.

In general, natural inclusion functions are not minimal, but many functions can be modified in order to satisfy the conditions in the following theorem and then their natural inclusion functions are minimal. Proofs and examples can be found in [23].

DEFINITION 2. An inclusion function $[\mathbf{g}]$ for $\mathbf{g}$ is convergent if, for any sequence of boxes $[\mathbf{x}](k)$,

$$\lim_{k\to\infty} |[\mathbf{x}](k)| = 0 \Rightarrow \lim_{k\to\infty} [g]([\mathbf{x}](k)) = 0, \tag{6}$$

with $|[\mathbf{x}](k)|$ being the volume of the box $[\mathbf{x}](k)$.

THEOREM. If $\mathbf{g}$ involves only continuous operators and continuous elementary functions then $[\mathbf{g}]$ is convergent. If, furthermore, each of the variables $\mathrm{x}_1, \ldots, \mathrm{x}_\mathrm{d}$ occurs at most once in the formal expression of $\mathbf{g}$, then $[\mathbf{g}]$ is minimal.

The next important concept is contraction, which is needed for the definition of likelihood functions and the update step of the proposed filters. The contraction operation actually represents an optimization procedure that finds the smallest box which satisfies certain constraints. One elegant way of performing this optimization is by formulating it as a constraint satisfaction problem (CSP). The CSP [23], often denoted by$\mathcal{H}$, can be written as

$$\mathcal{H}: (\mathbf{g}(\mathbf{x}) = 0,\ \mathbf{x} \in [\mathbf{x}]). \tag{7}$$

A common interpretation of (7) is: find the box enclosure of the set of vectors $\boldsymbol{x}$ belonging to a given prior domain $[\mathbf{x}]$ satisfying a set of m contraints $\mathbf{g} = (g_1, \ldots, g_m)^T$, with g_i a real valued function. The solution consists of all $\mathbf{x}$, that satisfy $\mathbf{g}(\mathbf{x}) = \mathbf{0}$ or written as a set:

$$\mathbb{S} = \{\mathbf{x} \in [\mathbf{x}] \mid \mathbf{g}(\mathbf{x}) = \mathbf{0}\}. \tag{8}$$

A contraction of $\mathcal{H}$ means replacing $[\mathbf{x}]$ by a smaller box $[\mathbf{x}]'$ under the constraint $\mathbb{S} \subseteq [\mathbf{x}]' \subseteq [\mathbf{x}]$. There are several methods to build a contractor for $\mathcal{H}$, e.g. by the Gauss elimination, Gauss-Seidel algorithm, and linear programming. In this work, however, we use constraint propagation (CP), sometimes referred as forward-backward propagation, for its suitability in the context of tracking problems. An example of a CP algorithm is given in the Appendix.

IV. THE SMC-PHD FILTER

Inspired by the works of Vo et al. [10] and Ristic et al. [12] on efficient SMC methods for the PHD filter, an improved SMC-PHD filter [12] is briefly presented in this paper to make it self-contained. The main improvement is a measurement steered particle placement for target birth. In addition, a target state and covariance matrix estimation without the need of clustering is introduced. The state of an individual object is represented by $\mathbf{x}_k \in \mathbb{R}^{n_x}$ and each measurement as $\mathbf{z}_k \in \mathbb{R}^{n_z}$. Assume that the transitional density $p(\mathbf{x}_k|\mathbf{x}_{k-1})$ is known through an evolution model $\mathbf{f}_k$, nonlinear in general, that is

$$\mathbf{x}_k = \mathbf{f}_k(\mathbf{x}_{k-1}) + \mathbf{w}_k, \tag{9}$$

with $\mathbf{w}_k$ a zero mean Gaussian white process noise.

The SMC-PHD filter consists of 6 steps, which are summarized in what follows. Here the particle set represents the target intensity $f_{k|k}(\mathbf{x})$ of the PHD filter, which corresponds to the multitarget state. Given from the previous time step we have the particle set:

$$\{(\mathbf{x}_i, w_i)\}_{i=1}^{N_k}, \tag{10}$$

with $\mathbf{x}_i \in \mathbb{R}^{n_x}$, w_i the corresponding weight and N_k denoting the number of particles, estimated at time step t_{k-1}. Recall that the integral over this intensity (or sum, if using particles) is the estimated expected number of targets and it is not necessarily equal to one. The implementation details using a particle PHD representation are presented below.

1) Predict Target Intensity

The resampled particle set gained from the previous step is denoted by $\{\mathbf{x}_i, w_i\}_{i=1}^{N_k}$. These particles represent the intensity over the state space. Another interpretation is that every particle represents a possible target state (called microstates in the language of thermodynamics), so that the prediction of the whole set can be modeled by applying a transition model to every particle and adding some noise to it. The weights remain unchanged at this step. In practical implementations this has the same effect as predicting the intensity distribution over the state space with a closed formula.

In order to avoid sampling a high number $N_{k,new}$ of newborn particles, the authors in [12] propose to sample newborn particles according to the measurement set $Z_{k-1} = \{\mathbf{z}_{k,1}, \ldots, \mathbf{z}_k, \mathrm{M}_{k-1}\}$ from the previous time step t_{k-1}. For each measurement $\mathbf{z}_{k-1,j},\ j = 1, \ldots, \mathrm{M}_{k-1}$, $N_{k,new}^j = N_{k,new}/M_{k-1}$ new particles $\tilde{\mathbf{x}}_i$ are drawn from a distribution $\beta_k(\mathbf{x}|\mathbf{z}_{k-1,j})$. In [12], $\beta_k(.|\mathbf{z}_{k-1,j})$ is constructed with the assumption that the state vector can be separated into a directly measured component vector and an unmeasured component vector. The measured component of the newborn particles can be sampled by inverting the measurement function while the unmeasured

components are sampled uniformly (see [12] for more details).

The weights of the newborn particles are set to

$$w_i = \frac{v_k}{N_{k,new}}, \quad i = N_k + 1, \ldots, N_k + N_{k,new}, \tag{11}$$

where v_k, as in [12], is a prior expected number of target births at time k. The predicted particle set contains the newborn and persistent particles and is $\{\tilde{\mathbf{x}}_i, w_i\}_{i=1}^{N_k+N_{k,new}}$.

2) Compute Correction Term

For all new measurements $\mathbf{z}_j$, with $j = 1, \ldots, m_k$ compute

$$\lambda_{k|k-1}(\mathbf{z}_j) = \lambda_c(\mathbf{z}_j) + \sum_{i=1}^{N_k+N_{k,new}} p_k(\mathbf{z}_j \mid \tilde{\mathbf{x}}_i) p_k^D(\tilde{\mathbf{x}}_i) w_i. \tag{12}$$

3) Update

Given m_k new measurements the update of the state intensity is realized through a correction of the individual particle weights. For every particle $(\mathbf{x}_i, w_i)$, with $i = 1, .., N_k + \mathrm{N}_{k,new}$ set:

$$\hat{w}_i = \left[(1 - p_k^D(\tilde{\mathbf{x}}_i)) + \sum_{j=1}^{m_k} \frac{p_k(\mathbf{z}_j \mid \tilde{\mathbf{x}}_i) p_k^D(\tilde{\mathbf{x}}_i)}{\lambda_{k|k-1}(\mathbf{z}_j)} \right] \cdot w_i. \tag{13}$$

4) Estimate Target States

To avoid a clustering step we use the methodology presented in [24]. First, compute the following weights for all new measurements $\mathbf{z}_j$, $j = 1, \ldots, m_k$ and all persistent particles, i.e., not the newborn particles $\tilde{\mathbf{x}}_i$, $i = 1, \ldots, N_k$.

$$w_{j,i} = \frac{p_k(\mathbf{z}_j \mid \tilde{\mathbf{x}}_i) p_k^D(\tilde{\mathbf{x}}_i)}{\lambda_{k|k-1}(\mathbf{z}_j)} \cdot w_i. \tag{14}$$

Then compute the following sum

$$W_j = \sum_{i=1}^{N_k} w_{j,i}, \tag{15}$$

which can be seen as a probability of existence for target j, similarly to the multitarget multi-Bernoulli filter [25]. For further analysis, only those j for which W_j is above a specified threshold τ are considered, i.e.,

$$\mathcal{J} = \{j | W_j > \tau, j = 1, \ldots, m_k\}. \tag{16}$$

For all $j \in \mathcal{J}$ the estimated point states are then:

$$\hat{\mathbf{y}}_j = \sum_{i=1}^{N_k} \tilde{\mathbf{x}}_i \ \cdot \ w_{j,i}. \tag{17}$$

Note that only targets that have been detected at time step t_k can be reported as present. This follows the lack of "memory" of a PHD filter. The full characteristics are discussed in [26, 27]. In practice τ is usually set as $\tau = 0.75$.

5) Estimate Covariance Matrices

For each estimated state $\hat{\mathbf{y}}_j$ compute its covariance matrix:

$$P_j = \sum_{i=1}^{N_k} w_{j,i} \left[(\tilde{x}_i - \hat{y})(\tilde{x}_i - \hat{y}_j)^T \right], \tag{18}$$

The matrix $\mathbf{P}_j$ is not an error covariance matrix in the sense of single-target Bayes filtering, but it characterizes the particle distribution of state $\hat{\mathbf{y}}_j$.

6) Resampling

Compute first the estimated expected number of targets

$$\eta_k = \sum_{i=1}^{N_k+N_{k,new}} \hat{w}_i. \tag{19}$$

Let N_{k+1} be the number of resampled particles, then any standard resampling technique for particle filtering can be used. Rescale the weights by η_k to get a new particle set $\{\mathbf{x}_i, \eta_k / N_{k+1}\}_{i=1}^{N_{k+1}}$.

V. DERIVATION OF THE BOX-PARTICLE PHD FILTER

A. From Particle to Box

Recall that applying particle filters to the PHD filter leads to a particle approximation of the intensity $f_{k|k}(\mathbf{x})$ by a set of N_k weighted random samples $\{(\mathbf{x}_i, w_i)\}_{i=1}^{N_k}$. The approximation can be written as

$$f_{k|k}(\mathbf{x}) \approx \sum_{i=1}^{N_k} w_i \delta_{x_i}(\mathbf{x}), \tag{20}$$

with $\delta_{x_i}(x)$ the Dirac delta function concentrated at $\mathbf{x}_i$. The sum (20) converges to $f_{k|k}(\mathbf{x})$, with $N_k \to \infty$ [28]. The number of particles used is a key issue to the overall filter performance. In general, the higher the number of particles, the better the approximation and with it the performance. However, a high number of particles leads often to a computationally demanding scenario. In [18] the authors presented a natural way to deal with the decrease of N_k by using boxes instead of point particles and combining particle filter techniques with interval analysis methods. Moreover, in [19] the authors propose to interpret box-particles as supports of uniform pdfs, so that (20) changes to

$$f_{k|k}(\mathbf{x}) \approx \sum_{i=1}^{N_k} w_i U_{[x_i]}(\mathbf{x}), \tag{21}$$

with $U_{[x_i]}(\mathbf{x})$ denoting the uniform pdf over the box $[\mathbf{x}_i]$.

Similarly to the scheme of the SMC-PHD filter the box-PHD filter can be summarized in 7 steps that are derived and presented in the following sections. Step 1 corresponds to the time update, steps 2–5 to the measurement update, and steps 6 and 7 to the resampling. A brief summary is also provided later in algorithm 1.

B. Time Update Step

Assume that from the previous time step we have the weighted box-particle set[2], $\{([\mathbf{x}_i], w_i)\}_{i=1}^{N_k}$ approximating the intensity (21), with $[\mathbf{x}_i] \in \mathbb{IR}^{n_x}$, w_i the corresponding weight, and N_k denoting the number of particles. The box-particle filter approximation of the PHD prediction equation (3) requires approximating two terms: the birth intensity $b(\mathbf{x}_k)$ and the persistent intensity.

1) Predict Target Intensity

As for the SMC-PHD filter, the approach in [12] is used here to approximate the newborn particles. Denote by $N_{k,new}$ the number of newborn particles to be sampled. For each measurement $\mathbf{z}_{k-1,j}$, $j = 1, \ldots, M_{k-1}$, $N_{k,new}^j = N_{k,new}/M_{k-1}$ new box-particles $[\tilde{\mathbf{x}}_i]$ are drawn from a distribution $\beta_k(\mathbf{x}|\mathbf{z}_{k-1,j})$, that is,

$$b(\mathbf{x}) \approx \sum_{j=1}^{M_k} \beta_k(\mathbf{x}|\mathbf{z}_{k-1,j}) \tag{22}$$

with

$$\beta_k(\mathbf{x}|\mathbf{z}_{k-1,j}) \approx \frac{1}{N_{k,new}^j} \sum_{i=1}^{N_{k,new}^j} U_{[\tilde{\mathbf{x}}_i]}(\mathbf{x}). \tag{23}$$

As described previously for the particle filter in Section IV, $\beta_k(.|\mathbf{z}_{k-1,j})$ is constructed by separating the state into a directly measured component and an unmeasured component. The measured components of the newborn box $[\tilde{\mathbf{x}}_i]$ in (23) are chosen by inverting each measurement box $[\mathbf{z}_{k-1,j}]$ while the unmeasured components are chosen according to a prior support. The weights of the newborn box-particles are set to

$$w_i = \frac{v_k}{N_{k,new}}, \quad i = N_k + 1, \ldots, N_k + N_{k,new}, \tag{24}$$

where v_k, as in [12], is a prior expected number of target births at time k.

Next, it remains to propagate the persistent box-particles, and hence to approximate the integral in (3), $\int p_s\, p(\mathbf{x}_k|\mathbf{x}_{k-1}) f_{k-1|k-1}(\mathbf{x}_{k-1}) \mathrm{d}\mathbf{x}_{k-1}$ can be approximated. Recall that the transitional density $p(\mathbf{x}_k|\mathbf{x}_{k-1})$ is known through an evolution model $\mathbf{f}_k$ (cf. (9)).

It is assumed furthermore that $\mathbf{w}_k$ is a bounded noise[3] in a box $[\mathbf{w}_k]$. According to [19] the following approximations are made with uniform pdfs (similarly to what is commonly used in the SMC-PHD time update step with Dirac functions):

$$\begin{aligned} &\int p(\mathbf{x}_k|\mathbf{x}_{k-1}) f_{k-1|k-1}(\mathbf{x}_{k-1}) \mathrm{d}\mathbf{x}_{k-1} \\ &\quad \approx\ w_i \sum_{i=1}^{N_k} U_{[\mathbf{f}_k]([x_i])+[\mathbf{w}_k]}(\mathbf{x}_k). \end{aligned} \tag{25}$$

Equation (25) means that the persistent box-particles are propagated using a transition function's inclusion function $[\mathbf{f}]$. Since the image of a box-particle $\mathbf{f}_k([\mathbf{x}_i])$ is not necessarily a box, an inclusion function has to be used.

The new set of predicted box-particles is the union of the newborn box-particles and the predicted persistent particle, that we denote $\{[\tilde{\mathbf{x}}_i], w_i\}_{i=1}^{N_k+N_{k,new}}$. The predicted PHD has the expression:

$$f_{k|k-1}(\mathbf{x}_k) \approx \sum_{i=1}^{N_k+N_{k,new}} w_i U_{[\tilde{\mathbf{x}}_i]}(\mathbf{x}_k). \tag{26}$$

C. Generalized Likelihood

In the measurement update step, an important challenge is how to implement the likelihood for the set of box-particles representing the PHD. For the M_k new measurements $\mathbf{z}_{k,j}$, in the context of this article, box measurements $[\mathbf{z}_{k,j}]$ are associated to them to model the noise. The sensor noise statistic is not modeled using a density (that in practice is often unknown). Instead, the only assumption that is made is that the sensor error range is known (in practice this information is known a priori). The likelihood terms $p([\mathbf{z}]|\mathbf{x})$, we are interested in, are called generalized likelihood. In [29], the generalized likelihood expression is derived and can be written

$$p([\mathbf{z}] \mid \mathbf{x}) = Pr\{\mathbf{h}(\mathbf{x}) + \mathbf{v} \in [\mathbf{z}]\}, \tag{27}$$

with $\mathbf{h}$ denoting the measurement model and $\mathbf{v}$ the stochastic noise associated to it (note that, without loss of generality, here we consider an additive noise). If we assume that the measurement model is deterministic and we neglect the effect of $\mathbf{v}$ (the expression of the generalized likelihood with the stochastic noise can be found in [30]), $p([\mathbf{z}]|\mathbf{x})$ has the form:

$$p([\mathbf{z}] \mid \mathbf{x}) = Pr\{\mathbf{h}(x) \in [\mathbf{z}]\} = U_{[\mathbf{z}]}(\mathbf{h}(\mathbf{x})), \tag{28}$$

Note that, in (28), for a more general problem, each measurement can be characterized using a weighted mixture of boxes (see [19]) to account for measurement noises with known statistics (e.g. Gaussian noise). In that case, the generalized likelihood can also be written as a weighted mixture of uniform pdfs.

D. Measurement Update Step

Using the set of box-particles $\{[\tilde{\mathbf{x}}_i], w_i\}_{i=1}^{N_k+N_{k,new}}$ approximating the predicted intensity $f_{k|k-1}(\mathbf{x}_k)$ and using the expression of the generalized likelihood (28), the terms in the correction step (5) are to be calculated.

2) Compute Correction Term

First, the denominator terms in the right-hand side of (5), denoted here $\lambda_{k|k-1}([\mathbf{z}_j])$, have the form:

$$\lambda_{k|k-1}([\mathbf{z}_j]) = \lambda_c([\mathbf{z}_j]) + \int p_D\, p([\mathbf{z}_j]|\mathbf{x}_k) f_{k|k-1}(\mathbf{x}_k) \mathrm{d}\mathbf{x}_k. \tag{29}$$

[2]For simplicity of notation, we skip the time index k for the particle in the rest of the paper when it is not needed.

[3]Without loss of generality, for simplicity noise $\mathbf{w}_k$ is restricted to be additive and bounded. In [19], the general case is considered with noise $\mathbf{w}_k$ approximated using a mixture of uniform pdfs.

Here, p_D is assumed constant. Using (26) and (28), the term $p([\mathbf{z}_j]|\mathbf{x}_k)f_{k|k-1}(\mathbf{x}_k)$ in (29) can be written as

$$p([\mathbf{z}_j]|\mathbf{x}_k)f_{k|k-1}(\mathbf{x}_k) \approx \sum_{i=1}^{N_k+N_{k,new}} w_i U_{[\mathbf{z}_j]}(\mathbf{h}(\mathbf{x}_k))U_{[\tilde{\mathbf{x}}_i]}(\mathbf{x}_k). \tag{30}$$

The term $U_{[\mathbf{z}_j]}(\mathbf{h}(\mathbf{x}_k))U_{[\tilde{\mathbf{x}}_i]}(\mathbf{x}_k)$ in (30) is also a constant function with a support being the following set $S_i \subset E_S$, where

$$S_i = \left\{\tilde{\mathbf{x}} \in [\tilde{\mathbf{x}}_i] \mid \mathbf{h}(\tilde{\mathbf{x}}_i) \in [\mathbf{z}_j]\right\}. \tag{31}$$

Equation (31) defines the solution set of a CSP and from its expression we can deduce that predicted box-particles $[\tilde{\mathbf{x}}_i]$ have to be contracted with respect to the measurement $[\mathbf{z}_j]$. Let us define the function $[h_{CP}]([\mathbf{x}], [\mathbf{z}])$ that returns the contracted version of $[\mathbf{x}]$ under the constraints given by the measurement function h. In this paper, $[h_{CP}]$ is obtained via the CP algorithm (see 23). An example of this contraction step is also given in the Appendix. Following this notation:

$$U_{[\mathbf{z}_j]}(\mathbf{h}(\mathbf{x}_k))U_{[\tilde{\mathbf{x}}_i]}(x_k) \approx \frac{|[\hat{\mathbf{x}}_{i,j}]|}{|[\tilde{\mathbf{x}}_i]||[\mathbf{z}_j]|}U_{[\hat{\mathbf{x}}_{i,j}]}(\mathbf{x}_k), \tag{32}$$

where we denote $[\hat{\mathbf{x}}_{i,j}] = [h_{\mathrm{CP}}]([\tilde{\mathbf{x}}_i],\ [\mathbf{z}_j])$.

Consequently, (30) can be further developed into

$$p([\mathbf{z}_j]|\mathbf{x}_k)f_{k|k-1}(\mathbf{x}_k) \approx \sum_{i=1}^{N_k+N_{k,new}} w_i \frac{|[\hat{\mathbf{x}}_{i,j}]|}{|[\tilde{\mathbf{x}}_i]||[\mathbf{z}_j]|}U_{[\hat{\mathbf{x}}_{i,j}]}(\mathbf{x}_k). \tag{33}$$

Note that this result (33) is always true for box-particle filter implementations and can be interpreted as: the likelihood calculation requires 1) contraction for the box-particles, and 2) a likelihood value proportional to the ratio between the volume of the newly contracted box-particle and the original one.

Furthermore, using the expression (33), (29) can now be written in the form

$$\begin{aligned}\lambda_{k|k-1}([\mathbf{z}_j]) &\approx \lambda_c([\mathbf{z}_j]) \\ &\quad + p_D \sum_{i=1}^{N_k+N_{k,new}} w_i \int \frac{|[\hat{\mathbf{x}}_{i,j}]|}{|[\tilde{\mathbf{x}}_i]||[\mathbf{z}_j]|}U_{[\hat{\mathbf{x}}_{i,j}]}(x_k)\mathrm{d}x_k \\ &= \lambda_c([\mathbf{z}_j]) + p_D \sum_{i=1}^{N_k+N_{k,new}} w_i \frac{|[\hat{\mathbf{x}}_{i,j}]|}{|[\tilde{\mathbf{x}}_i]||[\mathbf{z}_j]|}\end{aligned} \tag{34}$$

3) Update

By inserting the expression (30) inside the PHD update equations (4) and (5) the updated intensity can be approximated with box-particles according to

$$\begin{aligned}f_{k|k}(\boldsymbol{x}_k) &\approx (1-p_D)\sum_{i=1}^{N_k+N_{k,new}} w_i U_{[\tilde{\mathbf{x}}_i]}(\mathbf{x}_k) \\ &\quad + \sum_{j=1}^{M(k)}\sum_{i=1}^{N_k+N_{k,new}} w_i \frac{p_D U_{[\mathbf{z}_j]}(\mathbf{h}(\mathbf{x}_k))U_{[\tilde{\mathbf{x}}_i]}(\mathbf{x}_k)}{\lambda_{k|k-1}([\mathbf{z}_j])} \\ &\approx (1-p_D)\sum_{i=1}^{N_k+N_{k,new}} w_i U_{[\tilde{\mathbf{x}}_i]}(\mathbf{x}_k) \\ &\quad + p_D \sum_{j=1}^{M(k)}\sum_{i=1}^{N_k+N_{k,new}} w_i \frac{|[\hat{\mathbf{x}}_{i,j}]|}{|[\tilde{\mathbf{x}}_i]||[\mathbf{z}_j]|\lambda_{k|k-1}([\mathbf{z}_j])}U_{[\hat{\mathbf{x}}_{i,j}]}(\mathrm{x}_k).\end{aligned} \tag{35}$$

Equation (35) means that, given M_k new measurements, the update of the state intensity is realized through the contraction step of the box-particles and $(N_k + N_{k,new})$. $(M(k) + 1)$ new box-particles approximate the updated intensity. The box-particle weights are updated according to two groups that reflect the two terms summed in (35):

$$\hat{w}_i = [(1-p_D)] \cdot w_i, \tag{36}$$

$$\hat{w}_i = \left[p_D \sum_{j=1}^{M(k)} \frac{|[\hat{\mathbf{x}}_{i,j}]|}{|[\tilde{\mathbf{x}}_i]||[\mathbf{z}_j]|\lambda_{k|k-1}([\mathbf{z}_j])}\right] \cdot w_i. \tag{37}$$

To avoid this approximation with a potentially huge quantity of box-particles, a strategy scoring each measurement is introduced in step 6.

4) Estimate Target States

To avoid a clustering step we use the methodology in [24] also presented in Section IV for the SMC-PHD implementation. First, using (37) we compute the following weights for all the new measurements $[\mathbf{z}_j],\ j = 1, \ldots, m_k$ and all the persistent box-particles $[\tilde{\mathbf{x}}_i]$ or uniform pdfs $\mathrm{U}_{|\tilde{\mathbf{x}}_i|} i = 1, \ldots, N_k$ (the newborn box-particles are not used in this calculation).

$$w_{j,i} = \frac{p_D|[\hat{\mathbf{x}}_{i,j}]|}{|[\tilde{\mathbf{x}}_i]||[\mathbf{z}_j]|\lambda_{k|k-1}([\mathbf{z}_j])} \cdot w_i. \tag{38}$$

Then compute the following sum

$$W_j = \sum_{i=1}^{N_k} w_{j,i}, \tag{39}$$

which can be seen as a probability of existence for target j, similarly to the multitarget multi-Bernoulli filter. For further analysis only those j are considered for which W_j is above a specified threshold τ, i.e.,

$$\mathcal{J} = \{j | W_j > \tau,\ j = 1, \ldots, m_k\}. \tag{40}$$

For all $j \in J$ the estimated point states are then:

$$\hat{\mathbf{y}}_j = \frac{1}{W_j}\sum_{i=1}^{N_k} \mathrm{mid}([\tilde{\mathrm{x}}_i]) \cdot w_{j,i}. \tag{41}$$

For all $j \in J$ the estimated box states are then:

$$[\hat{\mathbf{y}}_j] = \frac{1}{W_j}\sum_{i=1}^{N_k} [\tilde{\mathrm{x}}_i] \cdot w_{j,i}. \tag{42}$$

In (41) and (42) we added, in contrast to [12], the normalization term $\frac{1}{W_j}$ to receive more accurate state estimates when W_j is not practically one.

5) Estimate Covariance Matrices

Using the interpretation of box-particles as a mixture of uniform pdfs, the covariance matrix for each state is

computed as

$$\mathbf{P}_j = \sum_{i=1}^{N_k} \frac{w_{j,i}}{W_j} \left[(\text{mid}([\tilde{\mathrm{x}}_i]) - \hat{\mathrm{y}}_j)(\text{mid}([\tilde{\mathrm{x}}_i]) - \hat{\mathrm{y}}_j)^T + \mathbf{\Sigma}_{\mathbf{U_i}} \right], \tag{43}$$

with $\mathbf{\Sigma}_{\mathbf{U_i}}$ a diagonal matrix of the form

$$\mathbf{\Sigma}_{\mathbf{U_i}} = \begin{pmatrix} |([x_i])_1|^2/12 & & \mathbf{0} \\ & \ddots & \\ \mathbf{0} & & |([x_i])_{n_x}|^2/12 \end{pmatrix} \tag{44}$$

containing the standard derivations for the individual uniform pdfs. In (43) we added, in contrast to [12], the normalization term $\frac{1}{W_j}$ to receive more accurate covariance matrix estimates when W_j is not practically one. The matrix $\mathbf{P}_j$ is not an error covariance matrix in the sense of single-target Bayes filtering, but it characterizes the particle distribution of state $\hat{\mathrm{y}}_j$.

6) Contract Particles

It has been shown in (35) that each box-particle has to be duplicated and contracted by each measurement. To avoid this nondesirable number of contractions, we propose to contract each box-particle $[\tilde{\mathrm{x}}_i]$, $i = 1, \ldots, N_k + N_{k,new}$ with its corresponding measurement. The corresponding measurement is defined through:

$$[\mathbf{z}^i] = \arg \max_{w_{j,i}} \{[\mathrm{z}_j], w_{j,i} > 0\}. \tag{45}$$

If no $[\mathbf{z}^i]$ is found, the box-particle $[\tilde{\mathbf{x}}_i]$ is not contracted, else $[\tilde{\mathbf{x}}_i]$ is set to

$$[\hat{\mathrm{x}}_i] = [\mathbf{h}_{\mathrm{CP}}]([\tilde{\mathbf{x}}_i], [\mathbf{z}^i]). \tag{46}$$

More formally, denote by S_1 the set of box-particles $[\tilde{\mathbf{x}}_i]$, $i = 1, \ldots, N_k + N_{k,new}$ for which $[\mathbf{z}^i]$ exists and denote by S_2 the remaining box-particles. The posterior intensity $f_{k|k}(\mathbf{x}_k)$ given in (35) can be further approximated into the following mixture of $N_{\mathrm{k}} + N_{k,new}$ pdfs:

$$\begin{aligned} f_{k|k}(\mathbf{x}_k) \approx (1 - p_D) \sum\nolimits_{[\tilde{\mathbf{x}}_i] \in S_2} w_i U_{[\tilde{\mathbf{x}}_i]}(\mathbf{x}_k) \\ + p_D \sum\nolimits_{[\tilde{\mathrm{x}}_i] \in S_1} w_i \frac{|[\hat{\mathbf{x}}_i]|}{|[\tilde{\mathbf{x}}_i]||[\mathbf{z}^i]|\lambda_{k|k-1}([\mathbf{z}^i])} U_{[\hat{\mathbf{x}}_i]}(\mathbf{x}_k). \end{aligned} \tag{47}$$

Equation (47) is an approximation of the more robust but more computational demanding (35). In [30] a different approach has been presented which is more similar to (35).

7) Resampling

Compute first the estimated expected number of targets

$$\eta_k = \sum_{i=1}^{N_k + N_{k,new}} \hat{w}_i. \tag{48}$$

Let N_{k+1} be the number of resampled particles. As explained in [19], instead of replicating box-particles, which have been selected more than once in the resampling step, we divide them into smaller box-particles as many times as they were selected. Several strategies of subdivision can be used (e.g. according to the largest box face). In this paper we randomly pick a dimension to be divided for the selected box-particle. Next, rescale the weights by η_k to get a new particle set $\{[\mathbf{x}_i], \eta_k / N_{k+1}\}_{i=1}^{N_{k+1}}$.

The box-PHD filter is summarized as algorithm 1.

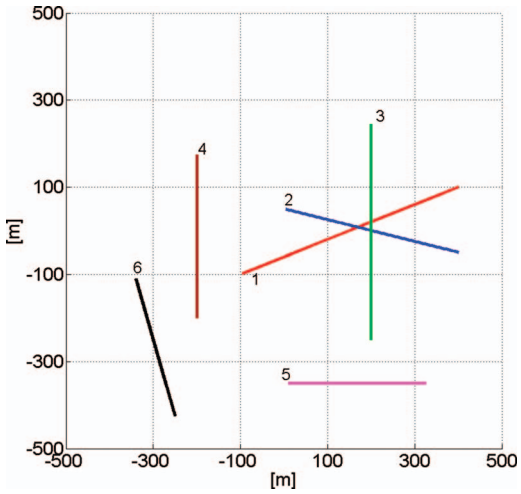

Fig. 1. Linear scenario used for performance evaluation. Six targets move inertially. Individual starting points of each target correspond to denoted target ID number. Targets 1 - 3 are present for all time steps. Target 4 is present between time step 15 and 90. Targets 5 and 6 are present between time step 30 and 75.

VI. NUMERICAL STUDIES

This section gives numerical studies for the proposed box-PHD filter algorithm. For comparison with traditional particle filter techniques we use a point particle SMC-PHD filter. As a performance measure the OSPA metric [21] is used for performance measure, together with the criteria for measuring the inclusion of the true state and the volume of the posterior pdf. The later two were introduced in [20, 30]. Both filters have been implemented in C++ in a similar way. In addition the Boost Interval Arithmetic Library [31] was used to handle interval datatypes.

A. Testing Scenario

We analyze the behavior of both filters in a demanding linear scenario. Herein six inertial moved targets are placed in an area $A = [-500,\ 500]\,\mathrm{m} \times [-500,\ 500]\,\mathrm{m}$. The unit is assumed to be meters. The state space is $S \subset \mathbb{R}^4$, where the first two components correspond to the x and y coordinates and the third and fourth correspond to their velocities. The measurement space consists of $[x]$ and $[y]$ measurements, so $\mathbf{Z} \subset \mathbb{IR}^2$. New measurements occur for the sake of simplicity every second. The measurement noise is white Gaussian noise with a standard deviation $\sigma_x = \sigma_y = 15\,\mathrm{m}$. The probability of detection is set equal for all states to $p_k^D([\mathbf{x}]) = 0.95$. Target placement and direction of movement are visualized in Fig. 1. Targets $1 - 3$ are present for all time steps. Target 4 is presented between time step 15 and 90. Targets 5 and 6 are present between time step 30 and 75. The whole scenario has a length of 100 time steps (seconds). The number of clutter

measurements is estimated following a Poisson distribution with the mean value $|A| \cdot \rho_A$.

Algorithm 1 The box-PHD filter

In: $\{([x_i], w_i)\}_{i=1}^{N_k}$, $\mathbf{Z}_k$, $\mathbf{Z}_{k-1}$
Out: $\{([\mathbf{x}_i], w_i)\}_{i=1}^{N_{k+1}}$, $\{[\hat{\mathbf{y}}_j], \hat{\mathbf{P}}_j\}$

1) Predict target intensity
   - For $I = 1, \ldots, N_k$ apply (50) to get $\tilde{\mathbf{x}}_i$.
   - Sample $N_{k,new}$ many new particles according to $\boldsymbol{Z}_{k-1}$
   - Weights for new particles are w_i (24)
2) Compute correction term
   - $\lambda_{k|k-1}([\mathbf{z}_j])$, according to (29)
3) Update target intensity
   - For every particle $([\tilde{\mathbf{x}}_i], w_i)$, with $I = 1, \ldots, N_k + N_{k,new}$ set the new weight according to (35).
4) Compute target states
   - Compute the set J (40)
   - For all $j \in J$: $[\hat{\mathbf{y}}_j] = \frac{1}{W_j} \sum_{i=1}^{N_k} w_{j,i} [\tilde{\mathbf{x}}_i]$ (42)
5) Compute covariance matrices
   - For all $j \in J$ compute $\mathbf{P}_j$ according to (43)
6) Contract boxes
   - $[\hat{\mathbf{x}}_i] = [\mathbf{h}_{\mathrm{CP}}]([\tilde{\mathbf{x}}_i], [\mathbf{z}])$ (46)
7) Resample
   - Use a resampling strategy with subdivision of boxes to get $\{([x_i], w_i)\}_{i=1}^{N_k+1}$

$$p(n_c) = \frac{1}{n_c!}(A \cdot \rho_A)^{n_c} \exp(-|A| \cdot \rho_A), \tag{49}$$

with $|A|$ denoting the volume of an observed area and ρ_A a parameter describing the clutter rate. For this scenario we used $\rho_A = 4 \cdot 10^{-6}$. Clutter measurements are generated by an independent and identically distributed (IID) process.

To initialize the particle cloud at time step $t_k = 0$, $N_0 \in \mathbb{N}^+$ particles are distributed uniformly across the state space S, e.g. $N_0 = 1000$. The weights are set to $w_j = 1/N_0$.

Assuming a constant velocity model in two dimensions the prediction of the persistent particles can be modeled by

$$[\tilde{\mathbf{x}}_i] = \begin{pmatrix} 1 & 0 & \Delta_t & 0 \\ 0 & 1 & 0 & \Delta_t \\ 0 & 0 & 1 & 0 \\ 0 & 0 & 0 & 1 \end{pmatrix} [\mathbf{x}_i] + [\boldsymbol{\nu}], \tag{50}$$

with $\Delta_t = t_k - t_{k-1}$ and $\boldsymbol{\nu}$ a 3σ interval of some white process noise, defined by a covariance matrix $\sum$. Hidden in (50) are inclusion functions for the individual dimension of the state space. A close look reveals that every variable only appears once (for each dimension) and that all operations are continuous, so these natural inclusion functions are minimal and the propagated boxes have minimal size. This fact holds for constant velocity models with arbitrary dimensions.

B. Performance Measures

Let us define $d^{(c)}(\mathbf{x}, \mathbf{y}) := \min(c, d(\mathbf{x}, \mathbf{y}))$ as the distance between $\mathbf{x}$, $\mathbf{y}$ cut off at $c > 0$, and π_l the set of permutations on $\{1, 2, \ldots, l\}$ for any $l \in \mathbb{N} = \{1, 2, \ldots\}$. For $1 \leq p \leq \infty$, $c > 0$, and arbitrary finite subsets $\mathbf{X} = \{\mathbf{x}_1, \ldots, \mathbf{x}_m\}$ and $\mathbf{Y} = \{\mathbf{y}_1, \ldots, \mathbf{y}_n\}$ of S, with $m, n \in \mathbb{N}_0$, the OSPA metric [21] is defined as

$$\bar{d}_p^{(c)}(\mathbf{X}, \mathbf{Y}) := \left(\frac{1}{n} \left(\min_{\pi \in \Pi_n} \left(\sum_{i=1}^{m} d^{(c)}(\mathbf{x}_i, \mathbf{y}_{\pi(i)})^p \right) + c^p(n-m) \right) \right)^{\frac{1}{p}}. \tag{51}$$

For the OSPA metric (51) we use directly the state estimates if using the SMC-PHD filter. To apply the OSPA metric to the box-PHD filter we use the point state estimates $\hat{\mathbf{y}}_j$ gained in (41) of the proposed algorithm. Alternatively, one can use the center points of the box states $\mathrm{mid}([\hat{\mathbf{y}}_j])$, which have the same values as $\hat{\mathbf{y}}_j$.

The inclusion value ρ measures whether the state vector is contained in the support of the posterior pdf, or in the case of the PHD filter, the posterior intensity. Given the ground truth for all targets $\mathbf{y}_l^*$, with l an index over the true number of targets, the inclusion for the SMC-PHD filter can be computed by evaluating

$$\rho_l^{\mathrm{SMC}} = \begin{cases} 1 & \exists j : \ (\hat{\mathbf{y}}_j - \hat{\mathbf{y}}_l^*)\, \mathbf{P}_j^{-1} (\hat{\mathbf{y}}_j - \hat{\mathbf{y}}_l^*)^T < \kappa \\ 0 & \text{otherwise.} \end{cases} \tag{52}$$

The condition in (52) checks if the ground truth is contained in the error ellipse defined by covariance matrix $\mathbf{P}_j$. The term κ defines the size of the error ellipse, e.g. use $\kappa = 11.8$ for a 3σ–ellipse in two dimensions [32]. The inclusion for the box-PHD filter is much simpler to compute: check if the ground truth $\mathbf{y}_l^*$ is contained in one of the state boxes $[\hat{\mathbf{y}}_j]$. If this is true the inclusion value is one, otherwise zero. Then ρ_l for the box-PHD filter is given by

$$\rho_l^{\mathrm{box}} = \begin{cases} 1 & \text{for } \mathbf{y}_l^* \in [\hat{\mathbf{y}}_j] \text{ and} \\ 0 & \text{otherwise.} \end{cases} \tag{53}$$

The volume criteria measures the spread of the particle distribution for a given state. To have a fair comparison between both filters we compute the volume for the SMC-PHD filter as

$$\nu_j^{\mathrm{SMC}} = \sqrt{6 \cdot \sqrt{\mathbf{P}_j(1,1)} + 6 \cdot \sqrt{\mathbf{P}_j(2,2)}}. \tag{54}$$

The volume in (54) is the square root of the widths of a box containing the 3σ–ellipse of state j. Note that we only consider here the position information, since the entries of $\mathbf{P}_j$ have different units. For the box-PHD filter the volume is computed as the square root of the widths of the box states, giving

$$\nu_j^{\mathrm{box}} = \sqrt{|[\hat{\mathbf{y}}_i](1)| + |[\hat{\mathbf{y}}_i](2)|}. \tag{55}$$

C. Simulations

1) *Accuracy Test*: In the first simulation we investigate the accuracy achieved with the box-PHD filter in comparison with the SMC-PHD filter. To do so we use

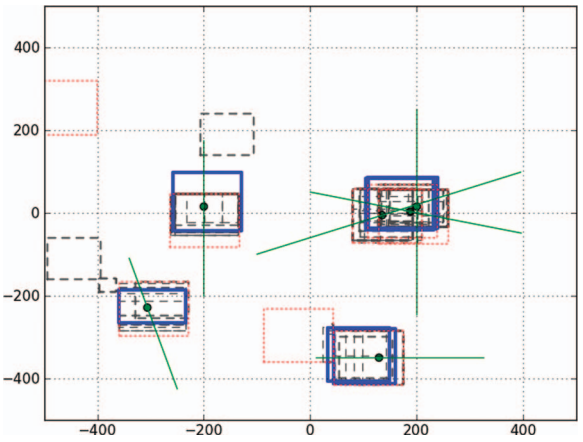

Fig. 2. Visualization of proposed box-PHD filter. Green solid lines are true target trajectories. Blue solid boxes correspond to projection of estimated box states into 2D. Box-particles are visualized as dashed black boxes, while red dotted boxes are measurements.

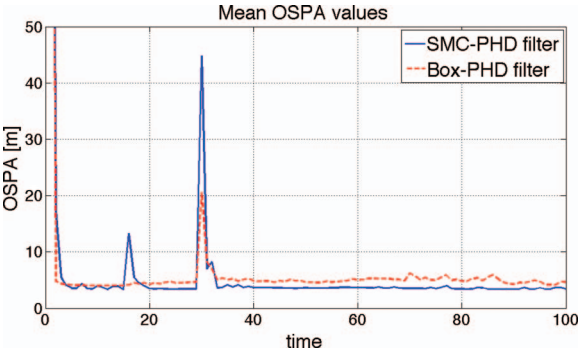

Fig. 3. Mean OSPA values for 1000 Monte Carlo trials on linear scenario for both filters.

the linear scenario described earlier. A visualization of the box-PHD filter for the linear scenario can be seen in Fig. 2. Fig. 3 shows the mean OSPA values achieved with both filters on the given scenario. We can observe that the OSPA values are in general very low. This means that the SMC-PHD filter and the box-PHD filter behave very well in this scenario. However, we can also observe that the box-PHD filter has a little higher values than the SMC-PHD filter. The authors of [20] already noticed that point estimates gained from box-particles can have a slight bias. Therefore they introduced two new measurement criteria – inclusion and volume. The mean results for 1000 Monte Carlo trials and all targets are shown in Figs. 4 and 5, respectively. It can be easily seen that the inclusion and volume values react to target appearance and target disappearance. In general we can say that the box-PHD filter has a higher volume then the SMC-PHD filter. This can be seen as a drawback of the box-particle technique. However, a closer look at the inclusion values reveals that the higher volume leads to better values for the inclusion criteria. So we can state that the SMC-PHD filter converges quickly to the solution and therefore it can happen sometimes that the true target state is not in the support of any covariance matrix $\mathbf{P}_j$. From an engineering

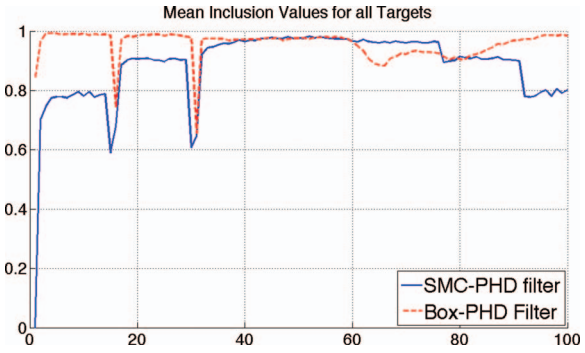

Fig. 4. Mean inclusion values for 1000 Monte Carlo trials and all targets on linear scenario without biased measurements for both filters.

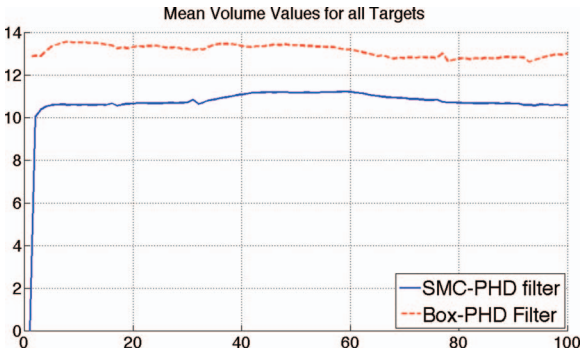

Fig. 5. Mean volume values for 1000 Monte Carlo trials and all targets on linear scenario without biased measurements for both filters.

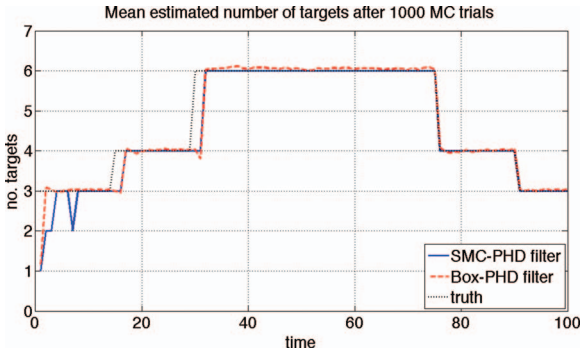

Fig. 6. Mean estimated number of states for 1000 Monte Carlo trials on linear scenario.

point of view both filters reach similar results in this scenario. This fact can also be seen in Fig. 6. Here, the estimated mean number of states is depicted. The curves of both filters are practically identical. Nevertheless, the number of particles needed for the box-PHD filter is much smaller in comparison with the SMC-PHD filter, which yields a better runtime shown in Table I. The mean speedup factor for the box-PHD filter is 10.9. The number of particles used in this scenario were 1875 for the SMC-PHD filter and only 63 for the box-PHD filter. Both filters have been implemented in C++. The box-PHD filter uses in addition the Boost Interval Analysis Library. Experiments were performed on an Intel Core 2 Duo (2.53 GHz) PC with 4GB RAM. Additional performance measures on the complexity of the approach have been

TABLE I
Mean Runtimes for Processing One Time Step

	Processing time (ms)	Speedup
SMC-PHD filter	10.3428	1.0
Box-PHD filter	0.95167	10.9

Note: Values computed over 1000 Monte Carlo trials and for all time steps of the linear scenario.

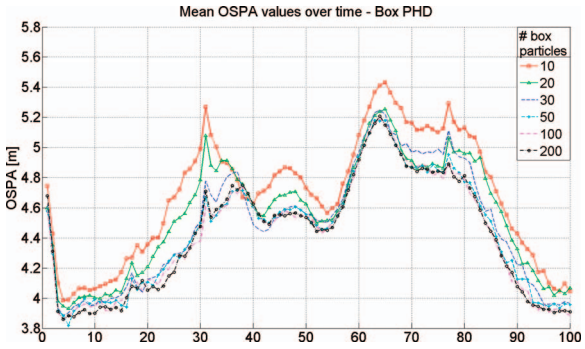

Fig. 7. Mean OSPA values for varying number of box-particles over time.

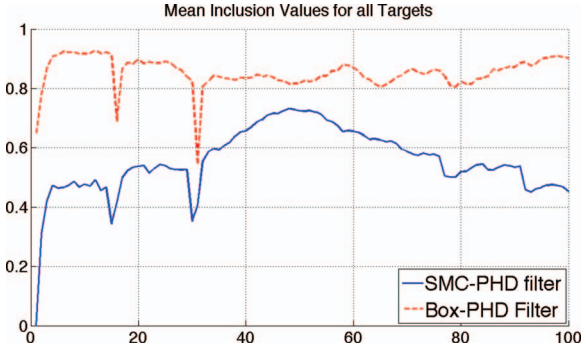

Fig. 8. Mean inclusion values for 1000 Monte Carlo trials and all targets on linear scenario with biased measurements for both filters.

published in [30]. Nevertheless, Fig. 7 shows mean OSPA values for 1000 Monte Carlo trials in the above scenario, where the number of box-particles used is varied. It can be seen that as few as 10 box-particles are needed in order to reach acceptable OSPA values. Worth mentioning is also that the maximum accuracy is already achieved by 50 box-particles for this scenario.

2) *Strong Bias*: In the next simulation we investigate the behavior of both filters when the sensor measurements have a strong bias, i.e., the bias is bigger than the white process noise of the sensor. The examples are similar to those considered in [33] and in [30]. The linear scenario is used again and we added to every measurement a bias of 30[m] for the x measurement and a bias of 10 for the y measurement. The volume of both filters does not change, which can be seen in Fig. 9. The inclusion criteria on the other hand change dramatically for the SMC-PHD filter; the value drops to values around 0.5[m], c.f. Fig. 8. This means that approximately 50% of the time the true target state is not within the posterior intensity of the filter. This

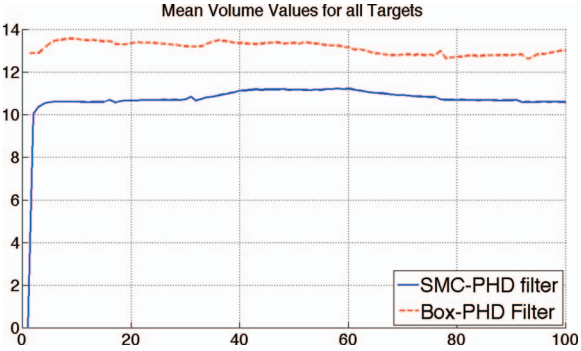

Fig. 9. Mean volume values for 1000 Monte Carlo trials and all targets on linear scenario with biased measurements for both filters.

indicates filter divergence, which is considered a catastrophic event in target tracking. The box-PHD filter, on the other hand, reaches values similar to the first simulation without bias. These results lead to the conclusion that the box-PHD filter outperforms the point SMC-PHD filter in scenarios with strongly biased measurements.

VII. CONCLUSION

In this paper we presented a novel technique for nonlinear multitarget tracking with a box-particle based filter, called the box-PHD filter. The theoretical backbone of this is the random finite set theory, which can be used to derive the general intensity filter equations. For the implementation, however, methods from interval analysis are used additionally to get a box-particle representation of the PHD filter. This representation allows a decrement of the number of particles needed. In our simulations we could reduce the number of particles by a factor of approximately thirty and reduce the computation time by a factor of approximately eleven. On the other hand, the accuracy of the filter was not remarkably reduced. Especially in the presence of strong bias we show that the box-PHD filter can outperform the SMC-PHD filter with point particles.

APPENDIX. CONTRACTION EXAMPLE

Assume the following scenario: a sensor measures azimuth α and range r in a local sensor coordinate system. The objective is to track a target in a global Cartesian coordinate system with these measurements. A measurement is then $\mathbf{z} = (\alpha, r)^T$, while the state is represented by $\mathbf{x} = (x, y)^T$. The point measurement function is defined as

$$\mathbf{z} = \mathbf{h}(x) = \begin{pmatrix} \arctan\left(\dfrac{y - y_0}{x - x_0}\right) & \text{Constraint 1} \\ \sqrt{(x - x_0)^2 + (y - y_0)^2} & \text{Constraint 2} \end{pmatrix}, \tag{56}$$

where $(x_0, y_0)^T$ is the sensor position in a global coordinate system. Equation (56) defines two constraints that will be used to contract a state box $[\mathbf{x}]$. Assuming box

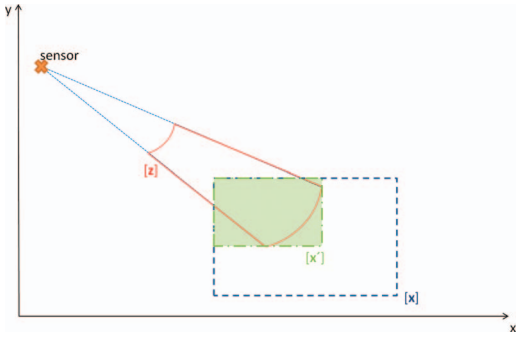

Fig. 10. Contraction example. Box $[\mathbf{x}]$ is contracted by measurement box $[\mathbf{z}]$. Result is green box $[\mathbf{x}']$.

measurements $[\mathbf{z}] = [\alpha] \times [r]$ and box states $[\mathbf{x}] = [x] \times [y]$, a contractor $[\mathbf{h}_{CP}]([\mathbf{x}]|[\mathbf{z}])$ based on constraint propagation [23] is given by the following algorithm:

---

0) Input: $[\mathbf{x}] = [x] \times [y]$, $[\mathbf{z}] = [\alpha] \times [r]$
Output: $[\mathbf{x}] = [x] \times [y]$

1) for Constraint 1 do:

$$[x] := [x] \cap [x_0] + \frac{[y] - [y_0]}{[\tan]([\alpha])} \quad (57)$$

$$[y] := [y] \cap [y_0] + ([x] - [x_0])[\tan]([\alpha]) \quad (58)$$

$$[\alpha] := [\alpha] \cap [\arctan]\left(\frac{[y] - [y_0]}{[x] - [x_0]}\right) \quad (59)$$

2) for Constraint 2 do:

$$[x] := [x] \cap [x_0] + \sqrt{[r]^2 - ([y] - [y_0])^2} \quad (60)$$

$$[y] := [y] \cap [y_0] + \sqrt{[r]^2 - ([x] - [x_0])^2} \quad (61)$$

$$[r] := [r] \cap \sqrt{([x] - [x_0])^2 - ([y] - [y_0])^2} \quad (62)$$

3) if the boxes $[\mathbf{x}]$ and $[\mathbf{z}]$ are changed return to step 1.

The box $[x_0] \times [y_0]$ represents the sensor position as a singleton. In practice we found it useful to stop this iteration after a finite number of loops, e.g. three, without any lack of performance. The quotient of the contracted box volume and the original box volume is used to calculate the likelihood. Fig. 10 visualizes the idea.

REFERENCES

[1] Bar-Shalom, Y., and Fortmann, T.
Tracking and Data Association. San Diego, CA: Academic, 1988.

[2] Fortmann, T., Bar-Shalom, Y., and Scheffe, M.
Sonar tracking of multiple targets using joint probabilistic data association.
IEEE Journal of Oceanic Engineering, **OE-8** (1983), 173–184.

[3] Reid, D. B.
An algorithm for tracking multiple targets. IEEE Transsactions on Automatic Control, **AC-24**, 6 (1979), 843–854.

[4] Mahler, R.
Multitarget Bayes filtering via first-order multitarget moments.
IEEE Transactions on Aerospace and Electronic Systems, **39**, 4 (2003), 1152–1178.

[5] Panta, K., Vo, B.-N., Singh, S., and Doucet, A.
Probability hypothesis density filter versus miltiple hypothesis tracking.
Proceedings of SPIE, Vol. 5429, 2004, pp. 284–295.

[6] Juang, R., and Burlina, P.
Comparative performance evaluation of GM-PHD filter in clutter.
In *Proceedings of the 12th International Conference on Information Fusion (FUSION '09)*, July 2009.

[7] Bar-Shalom, Y., Fortmann, and Scheffe, M.
Joint probabilistic data association for multiple targets in clutter.
In *Conference on Information Sciences and Systems*, 1980.

[8] Sidenbladh, H.
Multi-target particle filtering for probability hypothesis density.
In *International Conference on Information Fusion*, Cairns, Australia, 2003, pp. 800–806.

[9] Zajic, T., and Mahler, R.
A particle-systems implementation of the PHD multi-target tracking filter.
Proceedings of SPIE, Vol. 5096, *Signal Processing, Sensor Fusion Target Recognition XII*, 2003, pp. 291–299.

[10] Vo, B.-N., Singh, S., and Doucet, A.
Sequential Monte Carlo methods for multi-target filtering with random finite sets.
IEEE Transactions on Aerospace and Electronic Systems, **41**, 4, (2005), 1224–1245.

[11] Vo, B.-T., and Ma, W.-K.
The Gaussian mixture probability hypothesis density filter.
IEEE Transactions on Signal Processing, **55**, 11 (2006), 4091–4104.

[12] Ristic, B., Clark, D., Vo, B.-N., and Vo, B.-T.
Adaptive target birth intensity for PHD and CPHD filters.
IEEE Transactions on Aerospace and Electronic Systems, **48**, 2 (Apr. 2012), 1656–1668.

[13] Milanese, M., and Vicino, A.
Optimal estimation theory for dynamic systems with set membership uncertainty: An overview.
Automatica, **27**, 6 (1991), 997–1009.

[14] Combettes, P.
Foundations of set theoretic estimation.
Proceedings of the IEEE, **81**, 2 (1993), 182–208.

[15] Kruse, R., Schwecke, E., and Heinsohn, J.
Uncertainty and Vagueness in Knowledge Based Systems.
New York: Springer-Verlag, 1991.

[16] Smets, P.
Imperfect information: Imprecision and uncertainty. In A. Motto et al. (Eds.),
Uncertainty Management in Information Systems. Boston: KluwerAcademic Publishers, 1997, pp. 225–254.

[17] Anderson, B. D. O., and Moore, J. B.
Optimal Filtering. Upper Saddle River, NJ: Prentice-Hall, 1979.

[18] Abdallah, F., Gning, A., and Bonnifait, P.
Box particle filtering for nonlinear state estimation using interval analysis.
Automatica, **44** (2008), 807–815.

[19] Gning, A., Mihaylova, L., and Abdallah, F.
Mixture of uniform probability density functions for non linear state estimation using interval analysis.

In *Proceedings of the 13th International Conference on Information Fusion*, Edinburgh, UK, July 2010.

[20] Gning, A., Ristic, B., and Mihaylova, L.
A box particle filter for stochastic set-theoretic measurements with association uncertainty.
In *Proceedings of the 14th International Conference on Information Fusion*, Chicago, IL, July 2011.

[21] Schumacher, D., Vo, B.-T., and Vo, B.-N.
A consistent metric for performance evaluation of multi-object filters.
IEEE Transactions on Signal Processing, **56**, 8 (2008), 3447–3457.

[22] Mahler, R.
Multitarget Bayes filtering via first-order multitargets moments.
IEEE Transactions on Aerospace and Electronic Systems, **39**, 4 (2003), 1152–1178.

[23] Jaulin, L., Kieffer, M., Didrit, O., and Walter, E.
Applied Interval Analysis. New York: Springer, 2001.

[24] Ristic, B., Clark, D., and Vo, B.-N.
Improved SMC implementation of the PHD filter.
In *Proceedings of the 13th International Conference on Information Fusion*, Edinburgh, UK, July 2010.

[25] Vo, B.-T., Vo, B.-N., and Cantoni, A.
The cardinality balanced multi-target multi-Bernoulli filter and its implementations.
IEEE Transactions on Signal Processing, **57**, 2 (2009), 409–423.

[26] Erdinc, O., Willett, P., and Bar-Shalom, Y.
Probability hypothesis density filter for multitarget multisensor tracking.
In *Proceedings of the 8th International Conference on Information Fusion* (FUSION), Philadelphia, PA, July 2005.

[27] Erdinc, O., Willett, P., and Bar-Shalom, Y.
The bin-occupancy filter and its connection to the PHD filters.
IEEE Transactions on Signal Processing, **57**, 11 (2009), 4232–4246.

[28] Crisan, D., and Doucet, A.
A survey of convergence results on particle filtering methods for practinioners.
IEEE Transactions on Signal Processing, **50**, 3 (2002), 736–746.

[29] Mahler, R., and El-Fallah, A.
The random set approach to nontraditional measurements is rigorously Bayesian.
Proceedings of SPIE, Vol. 8392, *Signal Processing, Sensor Fusion, and Target Recognition XXI*, 2012, pp. 83 920D–83 920D–10. [Online]. Available: http://dx.doi.org/10.1117/12.919824.

[30] Gning, A., Ristic, B., and Mihaylova, L.
Bernoulli particle / box-particle filters for detection and tracking in the presence of triple measurement uncertainty.
IEEE Transactions on Signal Processing, **60**, 5 (2012), 2138–2151.

[31] Boost interval arithmetic library. [Online]. Available: www.boost.org/doc/libs/1_53_0/libs/numeric/interval/doc/interval.htm. Dec. 2006.

[32] Press, W., Flannery, B., Teukolsky, S., and Vetterling, W.
Numerical Recipes in C: The Art of Scientific Computing (2nd ed.). New York: Cambrige University Press, 1992.

[33] Ristic, B., Clark, D. E., and Gordon, N.
Calibration of multi-target tracking algorithms using non-cooperative targets.
IEEE Journal of Selected Topics in Signal Processing, **7**, 3 (June 2013), 390–398.

Marek Schikora received a BS (Vordiplom, 2006) and the MS (Diplom, 2008) in computer science from the University of Bonn, Germany. He is a Ph.D. student at the Computer Vision Group at the Technical University of Munich, Germany.

Since 2009 he has been a research scientist in the Sensor Data and Information Fusion Department at Fraunhofer FKIE, Germany, where he is leading a research team with a focus on aerial vision. His research is focused on sensor fusion, multitarget tracking and related computer vision topics, like image segmentation, object detection, and classification.

Amadou Gning received his PhD degree in the area of "technologies of information and systems" at the Université de Technologie de Compiègne, France in 2006.

He is currently working with the School of Computing and Communications, Lancaster University, United Kingdom. His interests are in the area of sensor data fusion and cover theoretical tools such as nonlinear filtering, sequential Monte Carlo methods, statistical signal processing, distributed sensor networks, and interval analysis.

Lyudmila Mihaylova (SM'08) is an Associate Professor with the University of Sheffield, Department of Automatic Control and Systems Engineering, United Kingdom. From 2006 to 2013 she was with the University of Lancaster, United Kingdom. Her interests are in the areas of nonlinear filtering, sequential Monte Carlo Methods, statistical signal processing, and sensor data fusion. Her work involves the development of novel Bayesian techniques, e.g. for high dimensional problems (including for vehicular traffic flow estimation and for image processing), localisation and positioning in sensor networks.

Dr. Mihaylova has published book chapters and numerous journal and conference papers in the areas of her research interests. She is the Editor-in-Chief of the *Open Transportation Journal* and an Associate Editor of the *IEEE Transactions on Aerospace and Electronic Systems* and *Elsevier Signal Processing Journal*. She is a member of the International Society of Information Fusion (ISIF). She has given a number of invited tutorials including for the COST-NEARCTIS workshop and is involved in the organization of international conferences/ workshops. Her research is funded by grants from the EPSRC, EU, MOD, and industry.

Daniel Cremers received the MS (diploma) degree in theoretical physics from the University of Heidelberg, Germany in 1997, and the PhD degree in computer science from the University of Mannheim, Germany, in 2002.

He spent two years as a postdoctoral researcher at the University of California, Los Angeles, and one year as a permanent researcher at Siemens Corporate Research, Princeton, NJ. From 2005 to 2009, he headed the Computer Vision Group at the University of Bonn, Germany. Since 2009, he has been a full professor at Technical University of Munich.

Dr. Cremers has received several awards, in particular, the Best Paper of the Year Award 2003 by the Pattern Recognition Society, the Olympus Award 2004, and the 2005 UCLA Chancellor's Award.

Wolfgang Koch (F'10) PD Dr. habil, studied physics and mathematics at RWTH Aachen, Germany.

He is head of the Dept. of Sensor Data and Information Fusion at Fraunhofer FKIE, a research institute active in defence and security.

Dr. Koch has published several handbook chapters and numerous journal/conference articles on fusion topics. For the *IEEE Transactions on Aerospace and Electronic Systems*, he is Associate Editor-in-Chief and Technical Editor. Moreover, he is Member of the Board of Directors of the International Society of Information Fusion. At Bonn University he holds a habilitation degree in applied computer science and gives regular lecture series on sensor data and information fusion. He initiated a series of annual IEEE workshops, *SDF: Sensor Data Fusion: Trends, Solutions, Applications*. In 2008, he was executive Chair of the 11th International Conference on Information Fusion, 2008, Cologne, Germany.